Journal of Quantitative Spectroscopy & Radiative Transfer 330 (2025) 109220

Contents lists available at ScienceDirect

Journal of Quantitative Spectroscopy and Radiative Transfer

journal homepage: www.elsevier.com/locate/jqsrt

Line-shape parameters of the oxygen first rotational triplet

M.A. Koshelev *, I.N. Vilkov, G.Yu. Golubiatnikov, A.Yu. Sekacheva, M.Yu. Tretyakov

A.V. Gaponov-Grekhov Institute of Applied Physics of the Russian Academy of Sciences, 46 Ulyanov Str., 603950, Nizhny Novgorod, Russia

ARTICLE INFO

Keywords:
Molecular oxygen
First rotational triplet
Line shape
Collision relaxation
Speed dependence effect
Transitions frequencies

ABSTRACT

A lines shape of the first triplet of rotational band of oxygen molecule was studied beyond the Voigt profile in the framework of the quadratic approximation of speed dependence of collision relaxation rate. Recordings of the lines broadened by O_2 and N_2 were obtained at room temperature using two fundamentally different spectrometers, in particular, a video spectrometer and a spectrometer with radio-acoustic detection of absorption. A set of line-shape parameters was determined based on the line recording analysis. Data accuracy and reliability was evaluated from a comparative analysis of the parameters obtained from different techniques and with previous data.

1. Introduction

Molecular oxygen being one of the main constituents of the Earth's atmosphere plays important role in atmospheric radiation absorption, in particular at millimeter (mm) and submillimeter (submm) waves, where the O_2 spectrum is one of the main components in radiation transfer models. In the subTHz region the spectrum is mainly formed by the magnetic-dipole lines of the $X^3\Sigma_g^-$ ground vibrational and electronic state: the fine-structure lines are responsible for the mm-wave absorption; the lines of the first and second rotational triplets form the shape of the subTHz part of the submm-wave region.

The line-shape parameters of the fine-structure lines are rather well known from previous studies (see [1] and references therein) including accurate frequencies, pressure broadening and shifts, line-mixing, their dependence on speed and temperature. The rotational submm lines are much less studied mainly due to the problem of the radiation sources in this frequency range sometimes referred to as "THz gap" [2]. A few previous experimental studies [3-7] revealed collisional broadening and shifting parameters and partly their temperature dependences. The line-shape model functions used in all these studies for spectra analysis neglected dependence of collision relaxation on the molecular speed (speed-dependence or SD effect). This may lead up to a few percent distortion of the line shape, whereas, modern remote sensing community requires more accurate simulation from propagation models [8].

This work is devoted to study of the SD effect on the shape of the O_2 lines of the first rotational triplet at room temperature and various pressures of pure oxygen and in its mixture with nitrogen. These lines are located at about 368, 425 and 468 GHz and correspond to transitions $J',N' \leftarrow J,N = 3,2 \leftarrow 1,1,\ 3,2 \leftarrow 1,2$ and $3,3 \leftarrow 1,2$ (N and J are rotational and total angular momentum quantum numbers), respectively. Two fundamentally different spectrometers (video and radio-acoustic ones) utilized for spectra recording cover together a pressure range of about 0.1–3 Torr. Section 2 provides the experimental details. The line-shape analysis of the experimental spectra is given in Section 3. Section 4 presents the results of the study and their discussion. Main results are summarized in the Conclusions.

2. Experimental details

The more various experimental methods used to obtain data, the higher the reliability of the data. Two fundamentally different spectrometers, in particular, the spectrometer with radio-acoustic detection (RAD spectrometer) [9] and the video spectrometer [10] were utilized in this study for recording the lines of the first O_2 rotational triplet. Herewith, the RAD spectrometer was used to study all three lines, and the 425-GHz line was additionally probed in pure oxygen using the video spectrometer. Both spectrometers are briefly described below. They were earlier involved in similar complementary studies of H_2O, O_2, and CO lines reported in [11-13], where more technical details and measurement methods can be found. The experimental information is summarized in Table 1.

A backward-wave oscillator (BWO) phase locked against a harmonic of the microwave synthesizer was employed in both spectrometers as a radiation source. Radiation frequency stability is determined by the GPS-tracked frequency and time standard SRS FS740.

* Corresponding author.
E-mail address: koma@ipfran.ru (M.A. Koshelev).

https://doi.org/10.1016/j.jqsrt.2024.109220
Received 27 September 2024; Accepted 11 October 2024
Available online 12 October 2024

Table 1
Experimental details.

		Video	RAD
Radiation source (BWO)		OB-32	OB-30, OB-32
Optical path length, m		4	0.1
Manipulation frequency, Hz		777	80
Frequency points per recording		251	151
Time per point, s		0.27	0.5
Number of averages		2	10 - 100
Temperature, C		26.0–27.0	24.7–25.6
Pressure range, Torr	O_2	0.1–1.0	0.38–2.87
	N_2	-	0.13–1.75
Number of pressure points		18	8–19
HWHM, MHz	Γ_D	0.465	0.4–0.53
	Γ	0.24–2.16	0.8–6.25
Fit quality	O_2	700–1000	1100–7100
	N_2	-	900–3800

A 10-cm long copper gas cell of the RAD spectrometer combined with a sensitive microphone and a 2-m long stainless steel cell of the video spectrometer were permanently connected to a vacuum system for a gas pumping and filling. The gas pressure in the cell was permanently monitored using MKS Baratron Type 626B gauges of 1-Torr and 10-Torr ranges. Declared accuracy of baratrons is 0.25 % of Reading. To avoid a distortion of the magnetic-dipole oxygen lines by the external magnetic fields (Zeeman effect), the RAD cell was shielded by two layers of annealed and carefully demagnetized permalloy and video spectrometer cell was wrapped by a permalloy tape. Temperature of the cells (slightly heated above the room temperature) was stabilized and constantly monitored by temperature sensors installed on the cell surface (Pt100, class 1/3 DIN with an uncertainty of ±0.14 K at near room-T). The oxygen and nitrogen gas samples with a specified purity better than 99.999 % were provided by a local supplier.

The spectra recording was performed using radiation frequency manipulation (a square-wave frequency modulating function with a precisely known and fixed deviation) and further demodulation of the spectrometer output signal by means of a lock-in amplifier with reference frequency equal to the manipulation frequency. The deviation was approximately equal to the line width. In the video spectrometer, the radiation passed through the cell was detected by a liquid He-cooled InSb bolometer. In the RAD spectrometer, the pressure variations caused by difference in the gas absorption at frequencies defined by the radiation frequency deviation was registered by a capacitive microphone.

A series of line profiles were recorded at several pressures (Table 1). Each line recording consisted of 151 frequency points for the RAD spectrometer and 251 points for the video spectrometer having an acquisition time of 0.5 s and 0.27 s per point, respectively. To achieve a sufficient signal-to-noise ratio for accurate line-shape study, the final spectrum at each pressure was obtained by averaging the number of repeated recordings. Typical recordings obtained using the video and RAD spectrometers are shown in Figs. 1 and 2.

3. Line profile analysis

A shape of the observed line depends on a modulation-demodulation type used for spectra acquisition. The true line shape is obtained if modulation of a radiation power is used. In this case the observed line shape $S(f)$ can be modeled as

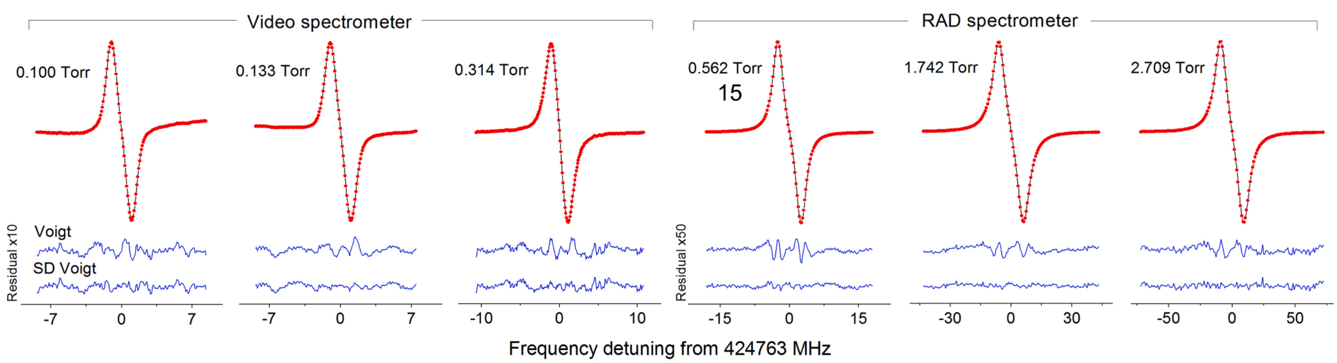

Fig. 1. Recordings of the 425-GHz line of $^{16}O_2$ from video (left) and RAD (right) spectrometers. Differences between experimental and fitted Voigt and SD Voigt profiles are shown below in magnified scale (note different vertical scales for video and RAD spectrometers). Pressure values are indicated next to the recordings.

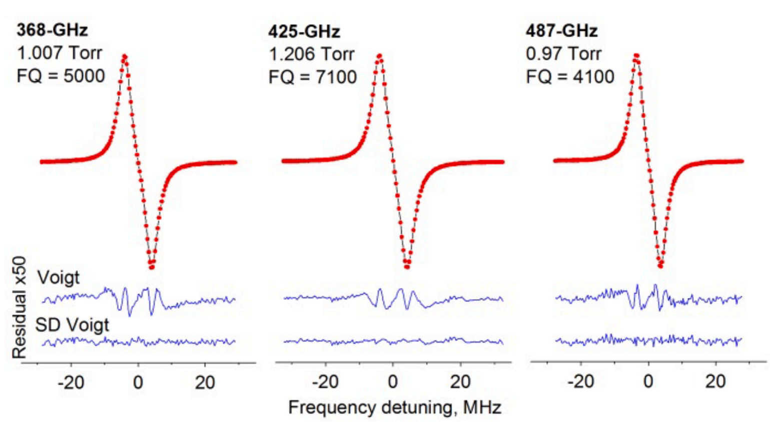

Fig. 2. Recordings of the 368-, 425-, and 487-GHz lines obtained in pure oxygen using RAD spectrometer. Frequency detuning is from 368,498.23, 424,763.0 and 487,249.26 MHz, respectively. Differences between the experimental and fitted Voigt and SD Voigt profiles are shown below in ×50 magnified scale. Pressure values and fit quality (FQ) are shown for each recording.

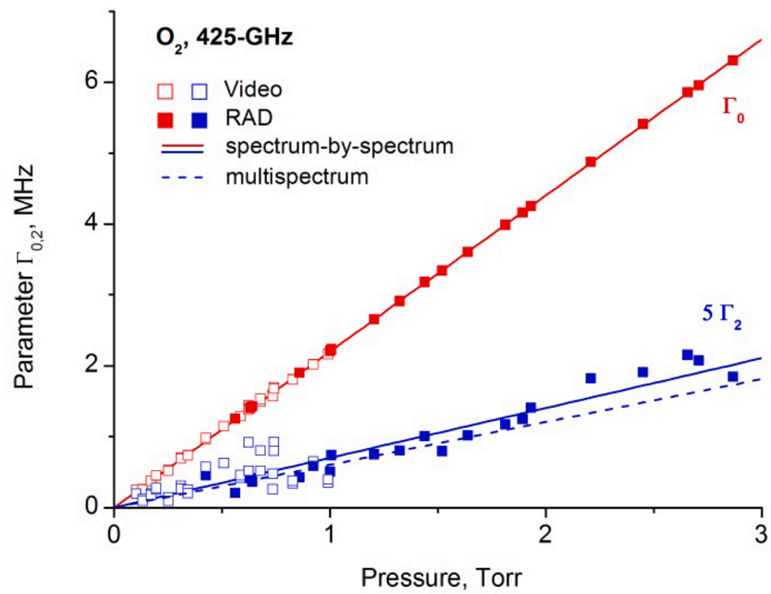

Fig. 3. Pressure dependence of the collisional line width Γ_0 and its speed-dependence Γ_2 (in ×5 magnified scale) for the self-broadened 425-GHz line. Data from video and RAD spectrometers are shown by open and filled symbols, respectively. Lines are results of linear regression of experimental points, obtained from spectrum-by-spectrum (solid line) and multispectrum (dashed line) analysis, respectively. For Γ_0 the solid and dashed lines merge.

$$S(f) = S_0(f)\cdot F(f), \tag{1}$$

where f is the frequency, $S_0(f)$ is the adjustable amplitude factor and $F(f)$ is the line-shape function (such as Lorentz or Voigt profile). In our case (radiation frequency manipulation (FMn) and further 1-f demodulation of the output signal by a lock-in amplifier), a differential line profile is observed and its shape $S_{FMn}(f)$ is modeled as

$$S_{FMn}(f) = S(f+d) - S(f-d), \tag{2}$$

where d is the deviation value. Its magnitude is precisely known and fixed for each line recording. The frequency manipulation method significantly reduces the spectrometer baseline. However, in some cases (mainly for the video spectrometer) a polynomial function (up to the third order) was added to the line shape model to take into account the remaining instrumental baseline. The amplitude factor $S_0(f)$, related to the frequency dependence of radiation power, was assumed to have linear frequency dependence $S_0(f) = S_0'\cdot\left(1 + S_0''\cdot(f - f_c)\right)$ for the entire recording range. Here f_c is a line center frequency, S_0' and S_0'' are adjustable parameters individual for each recording.

Spectra analysis was performed on a basis of two line shape models $F(f)$. The first one is the Voigt profile (Vp) which is characterized by the Doppler half-width Γ_D and collisional half-width Γ. The ratio Γ/Γ_D in our experiments varied approximately from 0.5 to 13. This simple model neglects the SD effect and shows a systematic (so called "w-shape") deviation in the vicinity of the line center (see residuals in Figs. 1 and 2). We used the Vp to compare properly the results of this study with

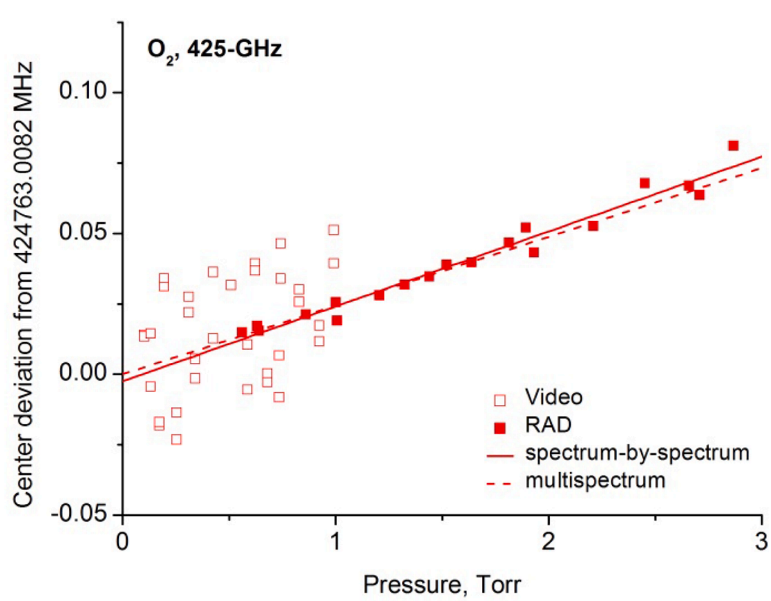

Fig. 4. Pressure dependence of the line center of the self-broadened 425-GHz line. Data from Video and RAD spectrometers are shown by open and filled symbols, respectively. Lines are results of linear regression of experimental points, obtained from spectrum-by-spectrum (solid line) and multispectrum (dashed line) analysis, respectively.

Table 2
Experimental parameters (in MHz/Torr) of the oxygen rotational triplet lines at 25.0 °C. Values in parenthesis are 1σ fit uncertainties. Total uncertainties are given in Table 5.

Parameter		3,2 ← 1,1	3,2 ← 1,2	3,3 ← 1,2
γ	O_2	2.2599(10)	2.1827(7)	2.1144(9)
	N_2	2.3135(13)	2.1803(14)	2.1217(18)
	Air*	2.3022(12)	2.1808(13)	2.1202(16)
δ	O_2	0.0143(14)	0.0244(9)	0.0257(9)
	N_2	0.0238(16)	0.0333(14)	0.0309(17)
	Air*	0.0218(16)	0.0314(13)	0.0298(15)
γ_0	O_2	2.2912(9)	2.1954(5)	2.1312(7)
	N_2	2.3441(15)	2.2053(18)	2.1596(24)
	Air*	2.3330(14)	2.2032(15)	2.1536(20)
γ_2	O_2	0.1644(15)	0.1208(11)	0.1276(12)
	N_2	0.2110(27)	0.1450(35)	0.1843(43)
	Air*	0.2012(25)	0.1399(30)	0.1724(37)
δ_0	O_2	0.0148(8)	0.0244(6)	0.0298(7)
	N_2	0.0180(23)	0.0337(12)	0.0360(30)
	Air*	0.0173(20)	0.0318(11)	0.0347(25)

* Calculated using formula $X_{Air} = 0.21 \cdot X_{O2} + 0.79 \cdot X_{N2}$, $X = \gamma, \delta$.

previous ones.

The SD effect was taken into account in the line profiles using a quadratic model [14,15], when Γ is assumed to have a quadratic dependence on the absorbing molecule speed υ:

$$\Gamma(\upsilon) = \Gamma_0 + \Gamma_2\left[\left(\frac{\upsilon}{\tilde{\upsilon}}\right)^2 - \frac{3}{2}\right],$$
$$\Delta(\upsilon) = \Delta_0 + \Delta_2\left[\left(\frac{\upsilon}{\tilde{\upsilon}}\right)^2 - \frac{3}{2}\right], \quad (3)$$

where $\Gamma_{0,2}$ and $\Delta_{0,2}$ are the pressure dependent parameters $\Gamma_{0,2} = \gamma_{0,2} \cdot p$, $\tilde{\upsilon} = \sqrt{2k_B T/m}$ is the most probable speed of the absorbing molecule of mass m at temperature T, and k_B is the Boltzmann's constant. The corresponding line shape model was a Hartman-Tran profile (HTp) in the limit of the quadratic speed-dependent Voigt profile (qSDVp) [16]. The speed dependence of pressure shifting was neglected, i.e. $\Delta(\upsilon) = \Delta_0 = \delta_0 \cdot p$.

Two approaches were used for the data analysis: (1) The multi-spectrum fitting procedure. It provides the simultaneous fitting of the model function to all experimental recordings of a chosen line at a given temperature. The expected linear dependence of collisional line shape parameters (broadening, shifting, and speed dependence parameter) on pressure is constrained in the model function. The procedure reduces the uncertainty of the results, which is related to the mutual correlation of the line shape and instrumental baseline parameters in the model function. (2) The spectrum-by-spectrum fitting approach. It implies a separate adjustment of each line shape parameter to each recording at a given pressure and following linear approximation of derived parameters.

The recordings from different spectrometers were analyzed separately. It is worth noting that both approaches demonstrated close results (Figs. 3 and 4), confirming the correctness of the model function and the minor effect of the spectrometer baseline on the results. Final values of the line shape parameters presented in the next sections are based on the multispectrum analysis as more reliable and physically correct procedure.

4. Results and discussions

4.1. Collisional broadening, shifting and speed dependence

The results of the spectrum-by-spectrum fit for the 425-GHz line of $^{16}O_2$ are shown in Fig. 3 for pressure dependence of Γ_0 and Γ_2 and in Fig. 4 for line center shifting Δ_0. Two datasets of experimental points from different spectrometers agree within the experimental uncertainties demonstrating the reliability of obtained data. The error bars are not presented for clarity of the figures. The average 1σ statistical uncertainties for the video and RAD spectrometer data are, respectively, 0.5 % and 0.08 % for Γ_0, 13 % and 5 % for Γ_2, and 1.8 kHz and 1.3 kHz for Δ_0. The final values of the line shape parameters are based mainly on more accurate and complete data from the RAD spectrometer, which are summarized in Table 2 for the temperature of 25 °C. Pressure broadening parameters γ and γ_0 and SD parameter γ_2 obtained at temperatures within 24.7–25.6 °C were recalculated to 25 °C using simple power law and temperature exponents n_γ from [6] (similarity of the exponents for γ, γ_0 and γ_2 for low N lines was previously demonstrated for the fine-structure lines [1]). The corrections did not exceed 0.15 % and the recalculation error caused by the temperature exponent uncertainty was at least ten times less and could be neglected. For the shifting parameters δ and δ_0 temperature dependence is not known (see [1]). It was neglected taking into account the narrow temperature range of the study. The air-broadening and shifting parameters presented in Table 2 were calculated from obtained data assuming validity of the binary collision approximation and air composition of 21 % of O_2 and 79 % of N_2.

Table 3
Broadening and shifting (in MHz/Torr) of the oxygen first rotational triplet lines measured in this study and from literature. Speed independent line shape profiles are assumed. Pressure broadening parameters are recalculated to 25 °C using power law and n_γ from [6].

Parameter		3,2 ← 1,1	3,2 ← 1,2	3,3 ← 1,2
γ	O_2	2.2599(10)	2.1827(7)	2.1144(9)
		2.25(3) [5]	1.60(16) [3]	2.09(3) [5]
		2.24(16) [7]	2.176(10) [4]	2.126(30) [7]
			2.168(14) [7]	
			2.02(6) [6]	
	N_2	2.3135(13)	2.1803(14)	2.1217(18)
			2.86(31) [3]	2.17(1) [5]
			2.200(20) [4]	1.87(39)* [7]
			2.11(9)* [7]	
			2.17(6) [6]	
	Air	2.3022(12)*	2.1808(13)*	2.1202(16)*
			2.60(28)* [3]	2.153(85)* [5]
			2.195(17)* [4]	1.92(30) [7]
			2.122(67) [7]	
			2.14(6)* [6]	
δ	O_2	0.0143(14)	0.0244(9)	0.0257(9)
		0.049(97) [7]	0.015(7) [7]	0.025(17) [7]
	N_2	0.0238(16)	0.0333(14)	0.0309(17)
			0.009(87)* [7]	0.003(105)* [7]
	Air	0.0218(16)*	0.0314(13)*	0.0298(15)*
			0.010(67) [7]	0.008(79) [7]

* Calculated using formula $X_{Air} = 0.21 \cdot X_{O2} + 0.79 \cdot X_{N2}$, $X = \gamma, \delta$.

Pressure broadening parameters from the present and previous studies are collected for comparison in Table 3 for all studied lines and in Fig. 5 for the 425-GHz line which is the most intense one of the triplet and has therefore been studied more often than two other lines. A good agreement of the data available for the 425-GHz line is seen except for the results of the earliest study [3], which overestimates N_2- and underestimates O_2-broadening.

The only previous experimental pressure shifting of the oxygen rotational lines were reported in [7] as estimation from broad-band spectra recordings obtained using a resonator spectrometer at atmospheric pressure. Despite this previous data is less accurate than the current one, both datasets are in good agreement in both sign and magnitude. Moreover, measured pressure shift values are within the assessed experimental limits ±40 kHz/Torr [4] and ±100 kHz/Torr [5]. The agreement of the data on both broadening and shifting parameters obtained using different spectroscopic methods at significantly different pressures indicates their high accuracy and reliability.

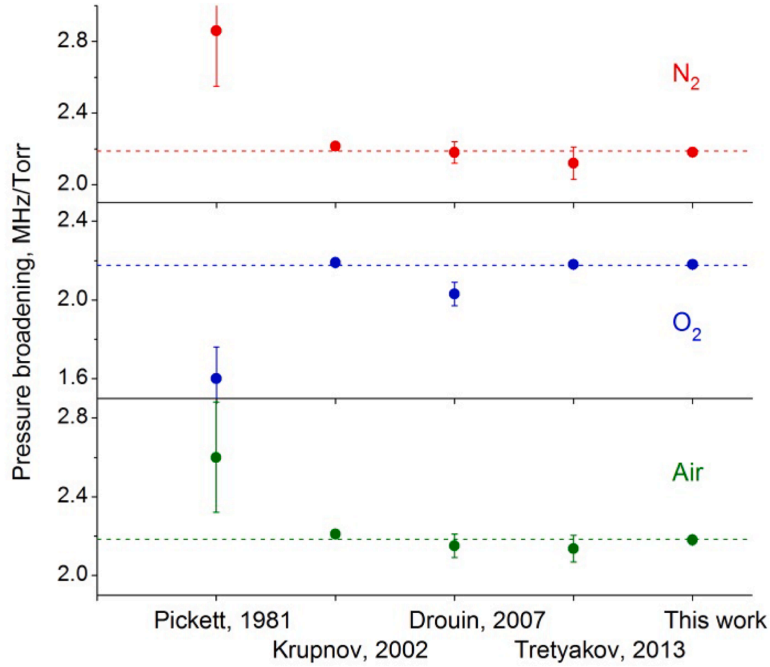

Fig. 5. Measurement history of pressure broadening parameters for the 425-GHz O_2 line. Dashed lines correspond to the weighted average values.

Table 4
Line centers (in MHz) of the oxygen first triplet. Uncertainties of our data correspond to 1σ error. Uncertainties for previous studies are presented as quoted in original papers.

N',J'–N,J	Observed	Obs.-calc.	Calculated*	Reference
3,2 ← 1,1	368,498.245(20)	0.0036	368,498.2414(73)	[5]
	368,498.2379(8)	**−0.0035**		This work
3,2 ← 1,2	424,763.80(20)	0.7849	424,763.0151(72)	[17]
	424,763.210(100)	0.1949		[18]
	424,763.030(14)	0.0149		[4]
	424,763.037(20)	0.0219		[19]
	424,763.0082(9)	**−0.0069**		This work
3,3 ← 1,2	487,249.270(30)	0.0028	487,249.2672(73)	[5]
	487,249.261(20)	−0.0062		[19]
	487,249.2625(11)	**−0.0047**		This work

* Obtained by effective Hamiltonian fitting to available experimental data in [12].

Table 5
Error budget of experimental parameters.

Parameter	Uncertainty (%)			
	Fit	Pressure	Temperature	Total
γ, γ_0	0.02–0.11	0.25	0.04	0.25–0.28
γ_2	0.9–2.4	0.25	0.04	0.93–2.4
δ, δ_0	2.4–12.8	0.25	–	2.4–12.8

4.2. *Line centers*

Measured pressure shifting allowed refining the zero pressure positions f_0 of the triplet lines. Table 4 collects the results of the current and all previous experiments in comparison with the latest calculated values [12]. The previously measured centers are seen to be mainly systematically higher than those obtained in this work that is likely due to ignoring a pressure shifting in the earlier studies.

4.3. *Uncertainty estimation*

To determine the total uncertainty of a particular line shape parameter, uncertainties of pressure and temperature reading were taken into account in addition to the fitting uncertainty as independent sources of potential errors. The total uncertainty is quoted for the data of the current study in Tables 2–4. Contribution of different error sources to the total uncertainty is presented in Table 5. Power law and n_γ from [6] were used for estimating the temperature uncertainty for γ, γ_0 and γ_2. Temperature dependence of pressure shift and related uncertainty were neglected.

A contribution of different errors to the total one is seen to be significantly different depending on a contribution of the corresponding collisional effect to the line shape. The collisional broadening is a first order effect forming the line shape in our study. Therefore, the fit uncertainty of γ and γ_0 is very small due to the high signal-to-noise ratio in experimental recordings and pressure uncertainty dominates in the total one. On the contrary, the pressure shifting of line center and speed dependence are the second order effects and fit uncertainty prevails over the others in the error budget of δ, δ_0 and γ_2. Total uncertainty of each parameter was calculated as a square root of the sum of squared relative errors assuming their independence.

Thus, the final uncertainty for γ and γ_0 is based on the values of total errors from Table 5 and constitutes 0.28 %. For δ, δ_0 and γ_2 the corresponding statistical fit uncertainties from Table 2 are an appropriate error evaluation.

Radiation frequency uncertainty is partially determined by the reference signal stability. A short-term relative stability of the SRS FS740 reference equipped with OCXO (ovenized crystal oscillator) timebase is claimed to be 10^{-11} which corresponds to about 4 Hz of absolute uncertainty of the radiation frequency. The pressure-related uncertainty of a line center determination was estimated to be <15 Hz based on a relative pressure uncertainty of 0.25 %. Thus, both aforementioned uncertainties are significantly small compared to the statistical one (about 1 kHz) and can be neglected.

Rotational and fine structure transitions of oxygen molecule $^{16}O_2$ form the close energy loops (Fig. 4.9 in [20]). It allows employing the Rydberg-Ritz principle for checking the accuracy of the retrieved line positions. Measured frequencies and shifts of the rotational lines allow

Table 6
Fine structure line positions and pressure self-shifts obtained as a difference of the frequencies and shifts of corresponding rotational transitions with the recently calculated values [12]. Errors are 1σ uncertainties.

Central frequency, MHz		Pressure shift δ, MHz/Torr	
Calculated from rotational lines	Calculated from [12]	Calculated from rotational lines	Calculated from [1]*
56,264.7703(17)	56,264.7738(3)	0.0101(23)	0.0012(10)
62,486.2543(20)	62,486.2520(3)	0.0013(18)	0.0012(10)

* Calculated from N-dependence $\delta(N) = 1.2 - 0.02{\cdot}N + 0.01{\cdot}N^2$ (kHz/Torr) obtained in [1].

calculating the corresponding parameters of the fine structure lines using the following loops of transitions:

(1,1 ← 1,2) = (3,2 ← 1,2) – (3,2 ← 1,1)

(3,3 ← 3,2) = (3,3 ← 1,2) – (3,2 ← 1,2)

The validity of extension of this principle to the pressure shifts has been discussed in [21-23], but no definite general conclusion was made. Thus the experimental verification seems interesting. Results of such calculations are presented in Table 6 in comparison with the data from recent experimental studies of positions [12] and pressure shifts [1] of the corresponding fine structure lines. An agreement of the compared values within the quoted uncertainties (or doubled in the case of the 1,1 ← 1,2 transition) demonstrates reliability of the measured frequencies and general applicability of the Rydberg-Ritz principle for these oxygen transitions.

5. Conclusions

Results of the first study of the speed dependence effect on a line shape of the first rotational triplet of oxygen in pure gas and in its mixture with nitrogen are reported. High quality recordings of the O_2 lines were obtained using two fundamentally different spectrometers at room temperature. Spectra analysis was performed using the speed dependent Voigt profile with the quadratic approximation of the SD effect. Reliably determined for the first time pressure shifting of the studied lines allowed refining their zero-pressure positions. The data consistency is well confirmed by the agreement of the results from different spectrometers of this and previous studies and the internal cross-check with the experimental results on the fine structure lines. The obtained data are expected to increase the accuracy of modeling the resonance oxygen absorption of subTHz radiation in models of radiation propagation in the atmosphere.

CRediT authorship contribution statement

M.A. Koshelev: Formal analysis, Investigation, Methodology, Writing – original draft, Writing – review & editing, Supervision. **I.N. Vilkov:** Data curation, Investigation. **G.Yu. Golubiatnikov:** Data curation, Formal analysis, Investigation, Methodology, Writing – review & editing. **A.Yu. Sekacheva:** Formal analysis. **M.Yu. Tretyakov:** Conceptualization, Supervision, Writing – original draft, Writing – review & editing.

Declaration of competing interest

The authors declare that they have no known competing financial interests or personal relationships that could have appeared to influence the work reported in this paper.

Acknowledgments

Experimental data were obtained using the research facilities "CKP-7" (USU №3589084). The study was supported by Russian Science Foundation (project no 22-72-10118, https://rscf.ru/en/project/22-72-10118/).

Data availability

Data will be made available on request.

References

[1] Koshelev MA, Vilkov IN, Galanina TA, Serov EA, Makarov DS, Tretyakov MYu. Temperature behavior of collisional parameters of oxygen fine-structure lines: O_2-O_2 case. J Quant Spectrosc Radiat Transfer 2023;298:108493.

[2] Pearson JC, Drouin BJ, Yu S. Instrumentation for THz Spectroscopy in the Laboratory and in Space. IEEE J Microw 2021;1(1):43–54. https://doi.org/10.1109/JMW.2020.3032454.

[3] Pickett HM, Cohen EA, Brinza DE. Pressure broadening of oxygen and its implications for cosmic background measurements. Astrophys J 1981;248:L49–51.

[4] Krupnov AF, Golubiatnikov GYu, Markov VN, Sergeev DA. Pressure broadening of the rotational line of oxygen at 425 GHz. J Mol Spectrosc 2002;215:309–11.

[5] Golubiatnikov GYu, Krupnov AF. Microwave study of the rotational spectrum of oxygen molecule in the range up to 1.12 THz. J Mol Spectrosc 2003;217:282–7.

[6] Drouin BJ. Temperature dependent pressure induced linewidths of $^{16}O_2$ and $^{18}O^{16}O$ transitions in nitrogen, oxygen and air. J Quant Spectrosc Radiat Transfer 2007;105:450–8.

[7] Tretyakov MYu, Koshelev MA, Vilkov IN, Parshin VV, Serov EA. Resonator spectroscopy of the atmosphere in the 350-500 GHz range. J Quant Spectrosc Radiat Transfer 2013;114:109–21.

[8] Turner E., Fox F., Mattiolo V., Cimini D. Literature Review on Microwave and Sub-millimetre Spectroscopy for MetOp Second Generation. Technical report NWPSAF-MO-TR-039; 2022.

[9] Tretyakov MYu, Koshelev MA, Makarov DS, Tonkov MV. Precise measurements of collision parameters of spectral lines with a spectrometer with radioacoustic detection of absorption in the millimeter and submillimeter ranges. Instrum Exp Tech 2008;51:78–88.

[10] Golubiatnikov GYu, Belov SP, Leonov II, Andrianov AF, Zinchenko II, Lapinov AV, et al. Precision subdoppler millimeter and submillimeter Lamb-dip spectrometer. Radiophys Quantum Electron 2014;56(8–9):599–609.

[11] Koshelev MA, Golubiatnikov GYu, Vilkov IN, Tretyakov Myu. Line shape parameters of the 22-GHz water line for accurate modeling in atmospheric applications. J Quant Spectrosc Radiat Transfer 2018;205:51–8.

[12] Koshelev MA, Golubiatnikov GYu, Vilkov IN, Tretyakov MYu. Molecular oxygen fine structure with sub-kHz accuracy. J Quant Spectrosc Radiat Transfer 2022;278:108001. https://doi.org/10.1016/j.jqsrt.2021.108001.

[13] Serov EA, Stolarczyk N, Makarov DS, Vilkov IN, Golubiatnikov GYu, Balashov AA, Koshelev MA, Wcislo P, Thibault F, Tretyakov MYu. CO-Ar collisions: ab initio model matches experimental spectra at a sub percent level over a wide pressure range. J Quant Spectrosc Radiat Transfer 2021;272:107807. https://doi.org/10.1016/j.jqsrt.2021.107807.

[14] Rohart F, Mader H, Nicolaisen HW. Speed dependence of rotational relaxation induced by foreign gas collisions: studies on CH_3F by millimeter wave coherent transients. J Chem Phys 1994;101(8):6475–86.

[15] Rohart F, Ellendt A, Kaghat F, Mäder H. Self and polar foreign gas line broadening and frequency shifting of CH_3F: effect of the speed dependence observed by millimeter-wave coherent transients. J Molec Spectrosc 1997;185(2):222–33.

[16] Ngo N, Lisak D, Tran H, Hartmann J-M. An isolated line-shape model to go beyond the Voigt profile in spectroscopic databases and radiative transfer codes. J Quant Spectrosc Radiat Transfer 2013;129:89–100.

[17] McKnight JS, Gordy W. Measurement of the submillimeter-wave rotational transition of oxygen at 424 kMc/sec. Phys Rev Lett 1968;21:1787–9.

[18] Steinbach W, Gordy W. Millimeter and Submillimeter Wave Spectrum of $^{18}O_2$. Phys Rev A 1973;8:1753–8.

[19] Drouin BJ, Yu S, Miller CE, Müller HSP, Lewen F, Brünken S, Habara H. Terahertz spectroscopy of oxygen, O_2, in its $^3\sum_g^-$ and $^1\Delta$ electronic states: THz Spectroscopy of O_2. J Quant Spectrosc Radiat Transf 2010;111:1167–73.

[20] Gordy W, Cook RL. Microwave molecular spectra. 3rd ed. New York: Wiley; 1984.

[21] Buffa G, Tarrini O. Comparison of pressure shift impact calculations with experimental results. J Molec Spectrosc 1983;101:271–7.

[22] Belli S, Buffa G, Tarrini O. On the extension of the Rydberg-Ritz principle to the collisional relaxation of molecular and atomic lines. Chem Phys Lett 1997;271:349–54.

[23] Krupnov AF, Skvortsov VA. To the nonadditivity mechanism of collisionally-perturbed spectral line widths and shifts. Russ Phys J 2001;44:339–47.